Australian Government

Australian Transport Safety Bureau

MH370 – Search and debris examination update

Released in accordance with section 25 of the *Transport Safety Investigation Act 2003*

Addendum

Page	Change	Date
18	Correction to Figure 11 caption to remove inconsistency with report text on Page 17.	2 Dec 2016

Executive summary

This report provides an update to the MH370 search area definition described in previous ATSB reports. It comprises further analysis of satellite data, additional end of flight simulations, a summary of the analysis of the right outboard wing flap, and preliminary results from the enhanced debris drift modelling.

For background information, please refer to the ATSB publications available online at www.atsb.gov.au/mh370:

- Definition of underwater search areas, 18 August 2014
- Flight Path Analysis Update, 8 October 2014
- Definition of Underwater Search Area Update, 3 December 2015.

The Australian Defence Science and Technology (DST) Group[1] conducted a comprehensive analysis of the Inmarsat satellite communications (SATCOM) data and a model of aircraft dynamics. The output of the DST Group analysis was a probability density function (PDF) defining the probable location of the aircraft's crossing of the 7th arc.

Details of this analysis and the validation experiments are available in the open source published book here: http://link.springer.com/book/10.1007/978-981-10-0379-0.

Additional analysis of the burst frequency offsets associated with the final satellite communications to and from the aircraft is consistent with the aircraft being in a high and increasing rate of descent at that time. Additionally, the wing flap debris analysis reduced the likelihood of end-of-flight scenarios involving flap deployment.

Preliminary results of the CSIRO's drift analysis indicated it was unlikely that debris originated from south of the current search area. The northernmost simulated regions were also found to be less likely. Drift analysis work is ongoing and is expected to refine these results.

---

[1] Formerly the Defence Science and Technology Organisation (DSTO).

Contents

# 7th arc burst frequency offset (BFO) analysis

The final satellite communication (Satcom) transmissions between the Inmarsat Ground station and 9M-MRO occurred at 00:19 on the 8th March 2014. These transmissions were the aircraft logging on to the Satcom system, likely after an interruption to the power that supplies the satellite data unit (SDU) – an integral part of the Satcom system.

The ground station Satcom logs recorded the burst timing offset (BTO) and the burst frequency offset (BFO) for each received message. A complete explanation of the BTO and BFO is provided in the ATSB publication, *MH370 – Definition of Underwater Search Areas, August 2014*.

The BFO is a function of the Doppler shifts imparted on the communication signal due to the motion of the satellite and the aircraft. The relationship is more complicated than a direct Doppler calculation because the aircraft software contains Doppler compensation that offsets the Doppler shift due to the aircraft motion. Although the aircraft attempts to compensate for its own motion, it does this under the assumption that the communications satellite is in notional geostationary orbit and it does not include the vertical component of the aircraft velocity.

Analysis of the BFO value can provide information about the relative motion between the satellite and the aircraft. Figure 1 shows all the BFO recordings from 9M-MRO. The comprehensive analysis provided by the Defence Science and Technology (DST) Group (*Bayesian Methods in the Search for MH370*) indicated that the aircraft was likely on a southerly heading at 18:39. From that point until 00:11, all the solutions of the analysis showed a continuing southerly track.

Figure 1: Recorded BFO values throughout the flight
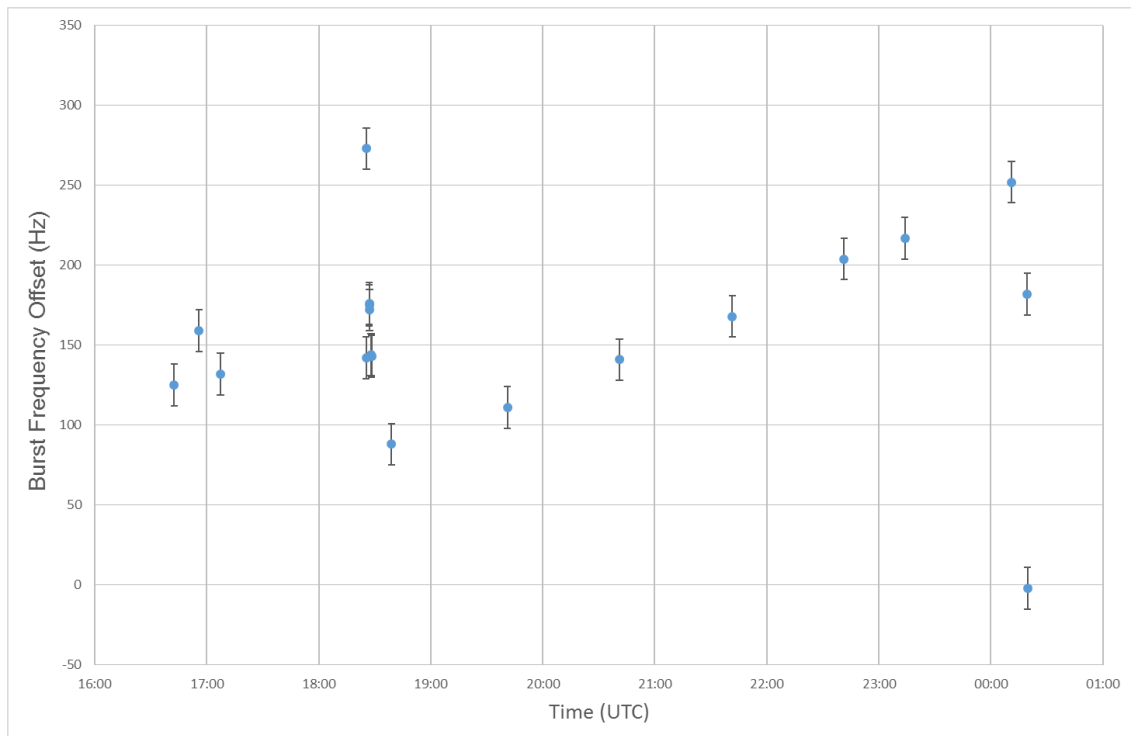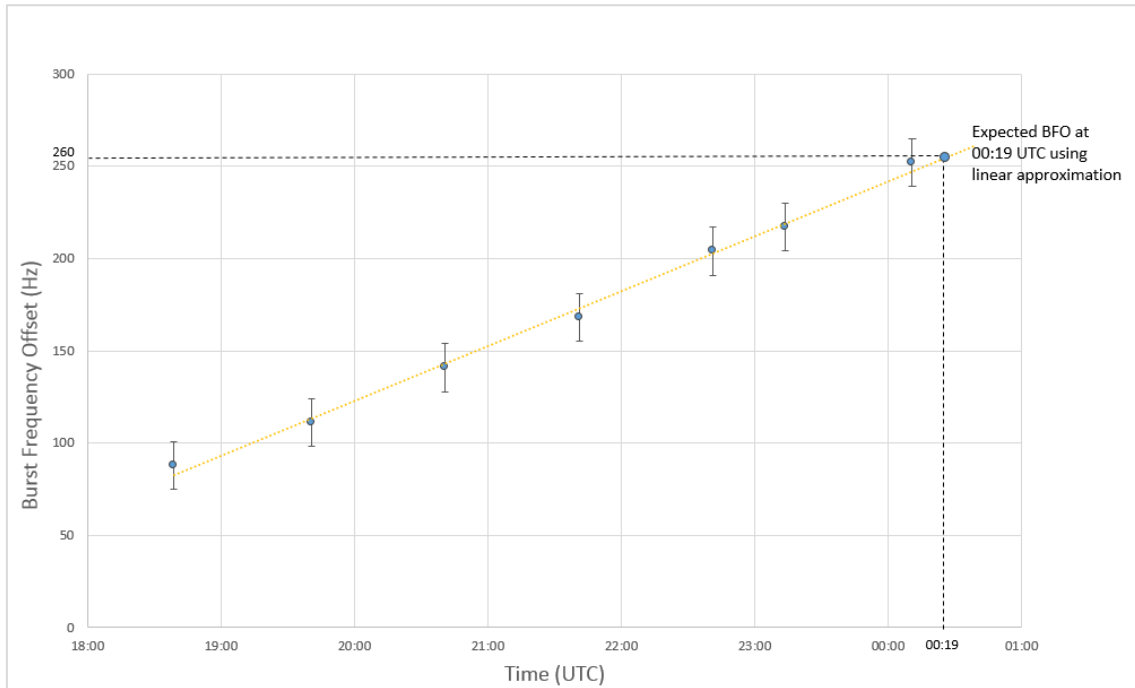

Source: ATSB

This graph illustrates the measured BFO recordings throughout the flight with the appropriate error bars on the measurements. After 18:39 the BFO values follow an approximately linear trend until the final two values at 00:19.

The trend of the BFO values from 18:39 until the 6th arc (00:11) is due to the change in location of the aircraft and can be linearly approximated (Figure 2). If this linear approximation is extrapolated to 00:19, and if neither the Satcom system nor the aircraft flight path were altered after 00:11, a BFO value of approximately 260 Hz would have been expected.

Figure 2: Linear approximation of the BFO values between 18:39 and 00:11

Source: ATSB

This graph illustrates 5 BFO values recorded between 18:39 and 00:11 and the linear approximation of the BFO at 00:19. The first 5 values correspond to the 2nd-6th arcs. During this time the aircraft is likely to be following a relatively constant southerly track. Continuing this linear trend to 00:19, a value of 260 Hz would be expected.

The recorded values of the BFO for the two messages at 00:19 were the following:

Table 1: Recorded BFO values at 00:19

Time	Burst Frequency Offset
00:19:29	182 Hz
00:19:37	-2 Hz

To explain this difference between the expected BFO value (260 Hz) and the recorded BFO values (Table 1), an examination was undertaken of the elements that contribute to the BFO.

This analysis includes a number of approximations, and the results should be interpreted as an approximate guide on the range of possible descent rates at the time of the last two SATCOM messages that were sent from 9M-MRO. DST Group intend to publish a more detailed version of the analysis in the near future. It should be noted that small refinements in the analysis may result in descent rate calculations that differ slightly from the values published here.

In the analysis it is assumed that there were no major changes to the satellite system between 00:11 and 00:19. Therefore the contributing elements consist of the:

- tolerance or error of the BFO
- direction of travel of the aircraft
- oven-controlled oscillator warm-up drift
- descent rate of the aircraft.

BFO tolerance or error

A statistical analysis of the BFO error from all the 20 previous flights of 9M-MRO identified that the distribution was approximately Gaussian (see DST Group book – link above) with a standard deviation of 4.3 Hz. ±3 standard deviations (12.9 Hz) is a conservative choice for the error.

Direction of flight

For any given speed, the estimated BFO differences can be plotted against the predicted heading of the aircraft (Figure 3). The maximum variation in the BFO differences based solely on change in direction is approximately 20 Hz.

Figure 3: Variation in estimated BFO differences at 00:19 for given track angles and groundspeed
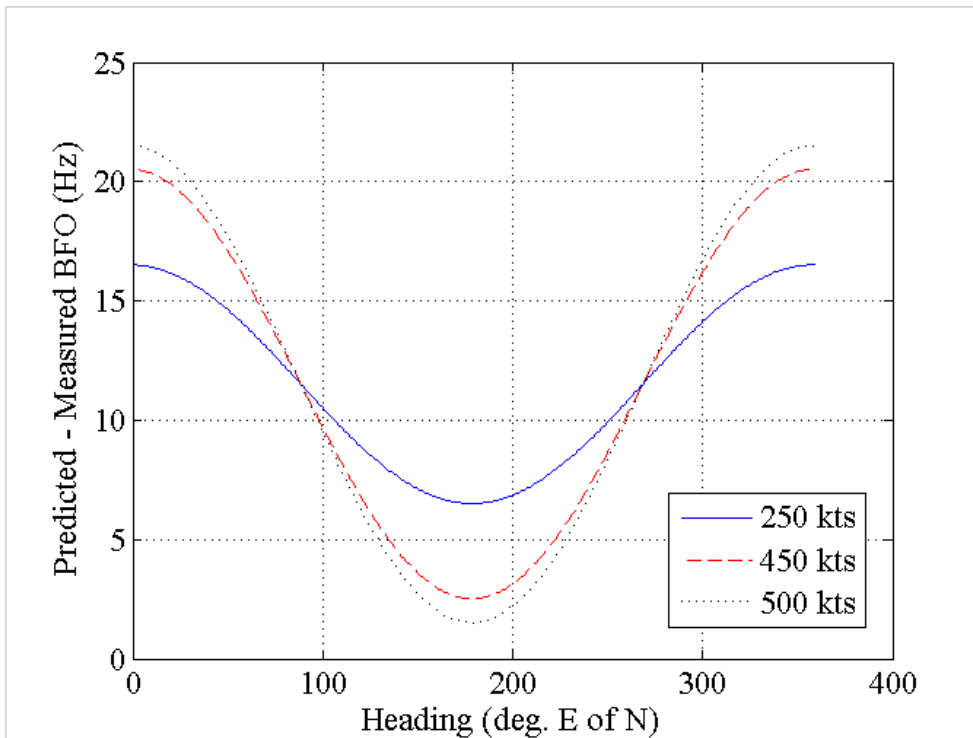
This graph indicates that the lowest BFO differences, and therefore the closest to our measured values, would be attained for any given speed by continuing in a southerly direction.

Oscillator warm-up drift

The oven-controlled crystal oscillator (OCXO) maintains the oscillator in the satellite data unit (SDU) at the design temperature. The performance of the OCXO in maintaining the correct temperature directly affects the transmitted frequency. When power is first applied to the SDU, the transient temperature variation associated with the OCXO warming-up causes a variation in the output frequency. This is referred to as warm-up drift.

To further understand this behaviour, the manufacturer of the SDU performed multiple power-up tests on several SDUs. It was observed that individual SDUs exhibit different warm-up drift characteristics. The differences were the magnitude of the frequency deviation, the time to reach steady state as well as the general shape of the curve.

Variations in the time in which the SDU (and OCXO) was not powered, prior to powering on, affected both the magnitude of the drift and the time taken for the frequency to stabilise, however the characteristic (or general shape of the curve) was not affected.

All available information indicated that, after power-up, the SDU in 9M-MRO exhibited a decay characteristic, represented in Figure 4. The values recorded shortly after power up would therefore be greater than the steady state value.

Figure 4: Representation of 9M-MRO SDU decaying warm-up characteristic (not to scale)
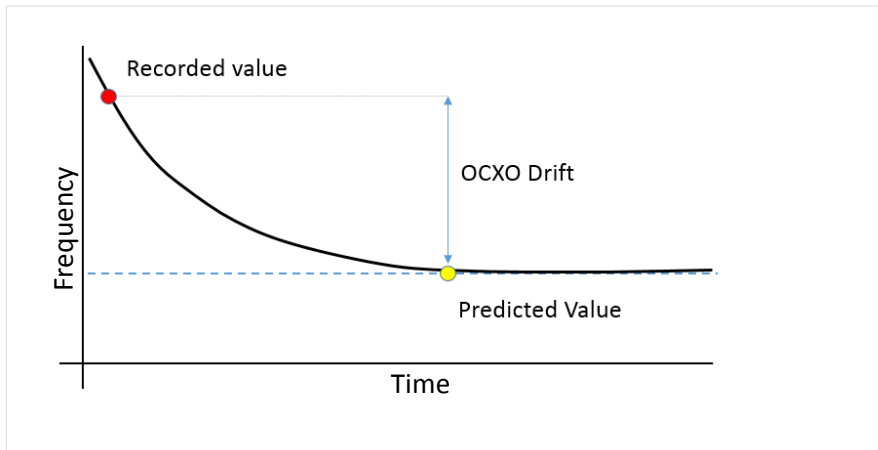
Source: ATSB

This graph illustrates the warm-up characteristic of the 9M-MRO SDU. After power is restored to the SDU, the OCXO drift results in BFO value being above the steady state value until the OCXO has stabilised.

The maximum OCXO drift value observed in the previous data of 9M-MRO was around 130 Hz and if the power interruption was sufficiently short, the OCXO drift could be negligible.

Descent rate

The remaining element to explain the difference in the predicted BFO value and the recorded BFO value is the descent rate of the aircraft. Analysis shows that at locations consistent with the search area and at the time of the last transmission, the descent rate affects the BFO value at -1.7 Hz per 100 ft/min.

Results of analysis

Due to the uncertainties associated with the end-of-flight scenario, it is not possible to define a specific descent rate from the recorded BFO values. Instead, using the limits of each contributing element, a range of possible descent rates, consistent with the recorded BFO values can be determined.

Case A and Case B below represent the boundary cases for the minimum descent rate and the maximum descent rate respectively. For each transmission at 00:19, Case A applies assumptions that reduce the required rate of descent to match the recorded BFO. Case B does the opposite and applies assumptions which increase the required rate of descent.

A. Minimum Descent Rate

    i.   Southerly direction,

    ii. Maximum positive error of measured BFO for 00:19:29 and 00:19:37 (~ 13 Hz),

    iii. No OCXO drift – very short duration power interruption.

B. Maximum Descent Rate

   i. Northerly direction,

   ii. Maximum negative error on measured BFO at 00:19:29 and 00:19:37 (~ -13 Hz),

   iii. Maximum OCXO drift – 130 Hz (as observed in other power-up logons of 9M-MRO).

Table 2 and Figure 5 following provide the resulting descent rates based on cases above for the log-on request at 00:19:29 and the log-on acknowledge at 00:19:37.

Table 2: Derived descent rate boundary cases

00:19:29 log-on request	Case A (minimum)	Case B (maximum)
Predicted BFO level flight	260 Hz	280 Hz
Measured BFO	182 Hz	182 Hz
Possible error (3 std dev.)	13 Hz	-13 Hz
OCXO Drift	0 Hz	130 Hz
Derived descent rate	260- (182+13) = 65 Hz (65 / 1.7) *100 ≈ 3,800 ft/min	280 - (182 - 13 - 130) = 241 Hz (241 / 1.7) *100 ≈ 14,200 ft/min

00:19:37 log-on ACK	Case A (minimum)	Case B (maximum)
Predicted BFO level flight	260 Hz	280 Hz
Measured BFO	-2 Hz	-2 Hz
Possible error (3 std dev.)	13 Hz	-13 Hz
OCXO Drift	0 Hz	130 Hz
Derived descent rate	260-(-2+13) = 249 Hz (249 / 1.7) *100 ≈ 14,600 ft/min	280 - (-2 - 13 - 130) = 425 Hz (425 / 1.7) *100 ≈ 25,000 ft/min

**Figure 5: Association of BFO differences to descent at 00:19**
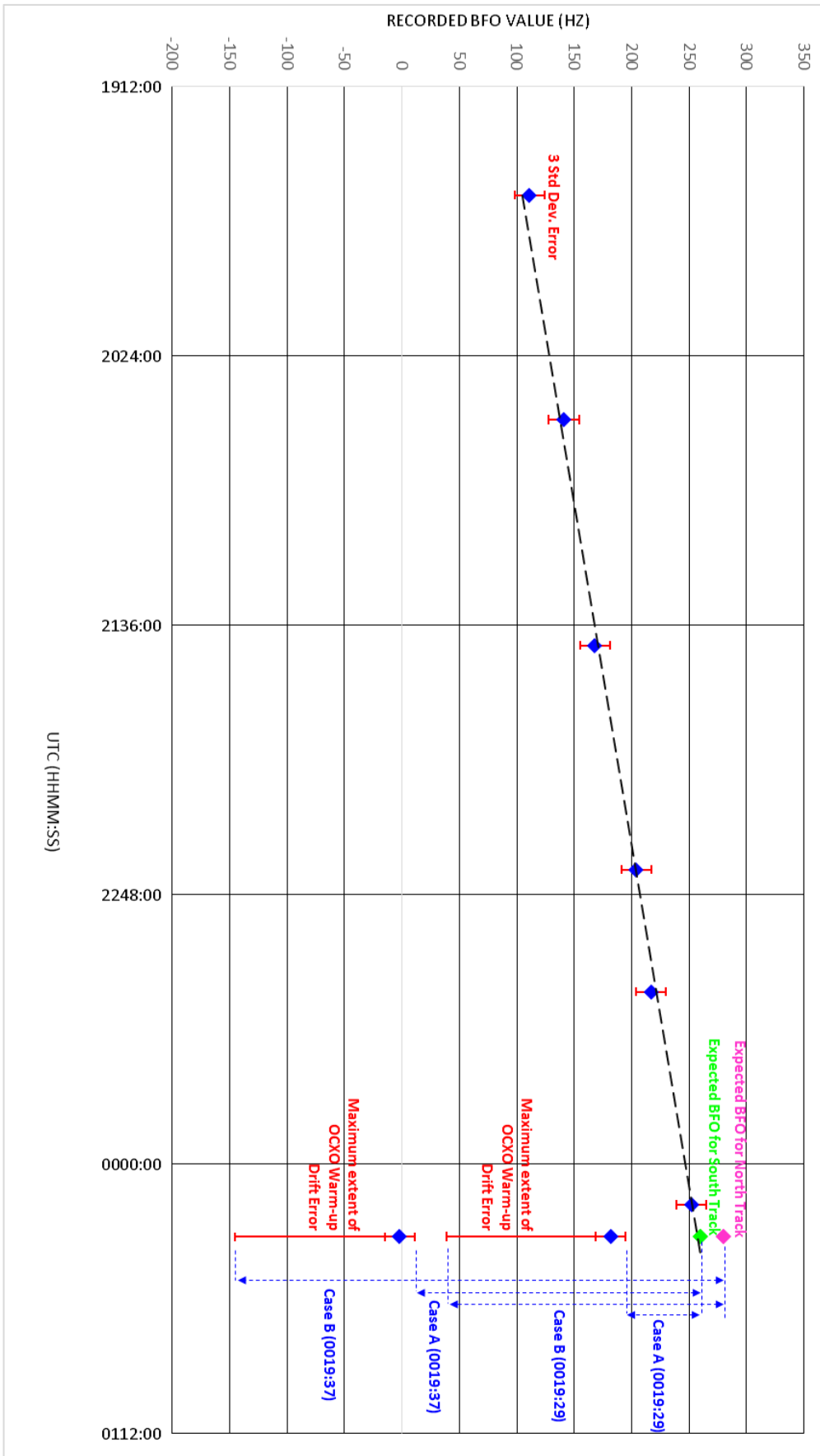
Source: ATSB

End of flight simulations

The ATSB report *MH370 – Definition of Underwater Search Areas, December 2015* outlined the previous simulations that the manufacturer had undertaken to assist in determining the aircraft's behaviour at the end of the accident flight.

In April 2016, the ATSB defined a range of additional scenarios for the manufacturer to simulate in their engineering simulator. Reasonable values were selected for the aircraft's speed, fuel, electrical configuration and altitude, along with the turbulence level.

The results of the simulation are presented in Figure 6. The results have all been aligned to the point two minutes after the loss of power from the engines. This is the theorised time at which the 7th arc transmissions would have been sent.

Figure 6: Results from simulated scenarios
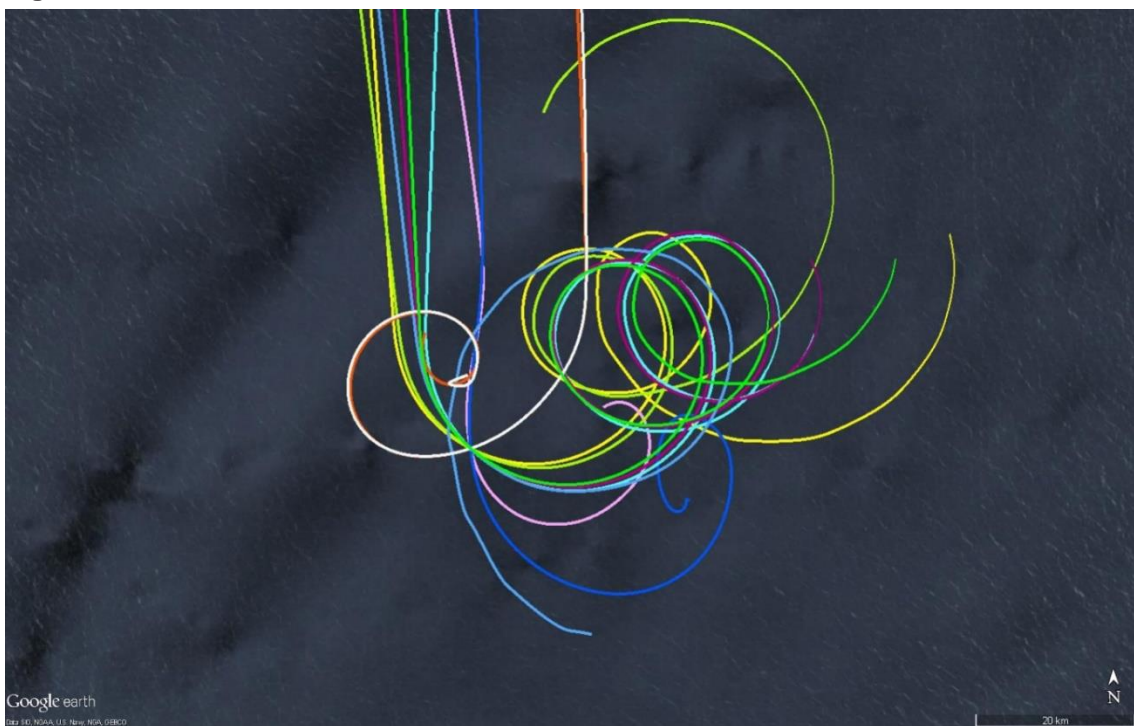
Source: ATSB

This figure illustrates the resulting flight paths from the simulations performed by the manufacturer and aligned at a point consistent with when the final BTO transmission may have occurred.

The simulations were completed in the manufacturer's engineering simulator. The engineering simulator uses the same aerodynamic model as a Level D simulator used by the airlines. The simulator is not a full motion simulator but instead is used when a high level of system fidelity is required. The appropriate firmware and software applicable to the accident aircraft can be loaded.

The results of the simulations were that:

- The aircraft was capable of travelling rearwards (from the direction of travel) approximately 21 NM.
- Simulations that experienced a descent rate consistent with the ranges and timing from the BFO analysis generally impacted the water within 15 NM of the arc.
- In some instances, the aircraft remained airborne approximately 20 minutes after the second engine flameout.

- In an electrical configuration where the loss of engine power from one engine resulted in the loss of autopilot (AP), the aircraft descended in both clockwise and anti-clockwise directions.
- In some simulations, the aircraft exhibited phugoid motion[2] throughout the descent.
- Simulations that exhibited less stable flight resulted in higher descent rates and impact with water closer to the engine flameout location. In some simulations, the aircraft's motion was outside the simulation database. The manufacturer advised that data beyond this time should be treated with caution.
- Some of the simulated scenarios recorded descent rates that equalled or exceeded values derived from the final SATCOM transmission. Similarly, the increase in descent rates across an 8 second period (as per the two final BFO values) equalled or exceeded those derived from the SATCOM transmissions. Some simulated scenarios also recorded descent rates that were outside the aircraft's certified flight envelope.
- The results of the scenarios, combined with the possible errors associated with the BTO values indicate that the previously defined search area width of ±40 NM is an appropriate width to encompass all uncontrolled descent scenarios from the simulations.

The simulated scenarios do not represent all possible scenarios, nor do they represent the exact response of the accident aircraft. Rather, they provide an indication as to what response the accident aircraft may have exhibited in a particular scenario. As such, the results are treated with caution, and necessary error margins (or safety factors) should be added to the results.

It was not possible to simulate all likely scenario conditions due to the limitations of the simulator. Specifically, flight simulators are unable to accurately model the dynamics of the aircraft's fuel tanks. In the simulator, when the fuel tank is empty, zero fuel is available to all systems fed from the tank. However, in a real aircraft, various aircraft attitudes may result in unusable fuel (usually below engine/APU inlets) becoming available to the fuel inlets for the APU/engines. If this resulted in APU start-up, it would re-energise the AC buses and some hydraulic systems. This could affect the trajectory of the aircraft. Similarly, the left and right engines may also briefly restart, affecting the trajectory.

---

[2] A long-period oscillation of pitch axis, perpetually hunting about level attitude and trimmed speed.

Drift modelling update

To assist with the underwater search for 9M-MRO, the Commonwealth Scientific and Industrial Research Organisation (CSIRO) undertook an analysis of existing ocean data from the Global Drifter Program[3]. The analysis used the behaviour of drogued and undrogued drifters[4], as well as numerical simulations using ocean models. The purpose of this work was to trace any recovered debris to its likely point of origin. However, a drifter's geometry and buoyancy is not generally representative of aircraft debris and it was considered that the drift characteristics might also be different. To account for this difference, the CSIRO engaged in field work, studying how aircraft debris moves through the water compared to drifters, with regard to wind and ocean currents. This data was incorporated into numerical simulations in order to predict the drift behaviour of aircraft debris with more confidence.

As part of the ongoing field testing, the drift behaviour of replica flaperons and other recovered aircraft parts is being assessed. Replica flaperons were constructed with dimensions and buoyancy approximately equal to that of the recovered flaperon (Figure 7), which was float-tested during the detailed examinations in France. The replica flaperons were deployed into a bay for short term tests during various weather conditions. Longer term tests were then performed in the open ocean. For comparison, undrogued drifters were deployed alongside the flaperons. Drogued drifters were also used, because they move predominantly with the currents, as opposed to wind and waves. Data for currents was then able to be subtracted from the flaperons' drift data so that wind and wave behaviour could be assessed in isolation.

Figure 7: Flaperon recovered from Reunion Island on 29 July 2015

Source: Bureau d'Enquetes et d'Analyses (BEA)

Field tests demonstrated that the replica flaperons drift similarly to undrogued drifters:

- In low wind conditions, the flaperons move slightly faster than undrogued drifters due to the energy absorbed from waves.

---

[3]   Visit www.aoml.noaa.gov/phod/dac/ for further details.
[4]   A drifter is a satellite-tracked buoy which either has a subsurface sea anchor attached (drogued) or not (undrogued).

- In higher winds, the energy absorbed from waves was less significant, and the flaperons' behaviour was analogous to the undrogued drifters'.

The replica flaperons presented their raised trailing edge to the wind, allowing waves to propel them in the wind direction. If waves tipped or turned the flaperons, the wind quickly reoriented them, so the direction of movement remained consistent.

Replicas of two other recovered items of debris drifted at a rate that was practically indistinguishable from undrogued oceanographic drifters in all wind conditions. Therefore, the trajectories of undrogued oceanographic drifters were valid for use in the analysis.

Preliminary results from the updated drift analysis indicated that the current search area was a possible origin for the recovered debris.

Using the collected field data, a new forward-tracking numerical simulation was performed. Within the simulation, flaperons were deployed on and around the current search area and allowed to drift freely. Results after 500 days of simulated drift are presented in Figure 8. For comparison, Figure 9 shows the results of a simulation where the original undrogued drifter model was used. By comparing the two figures, it can be seen that the flaperons generally moved further west within 500 days due to the extra speed at low winds.

Figure 8: Simulated location of flaperon-type drifters after 500 days
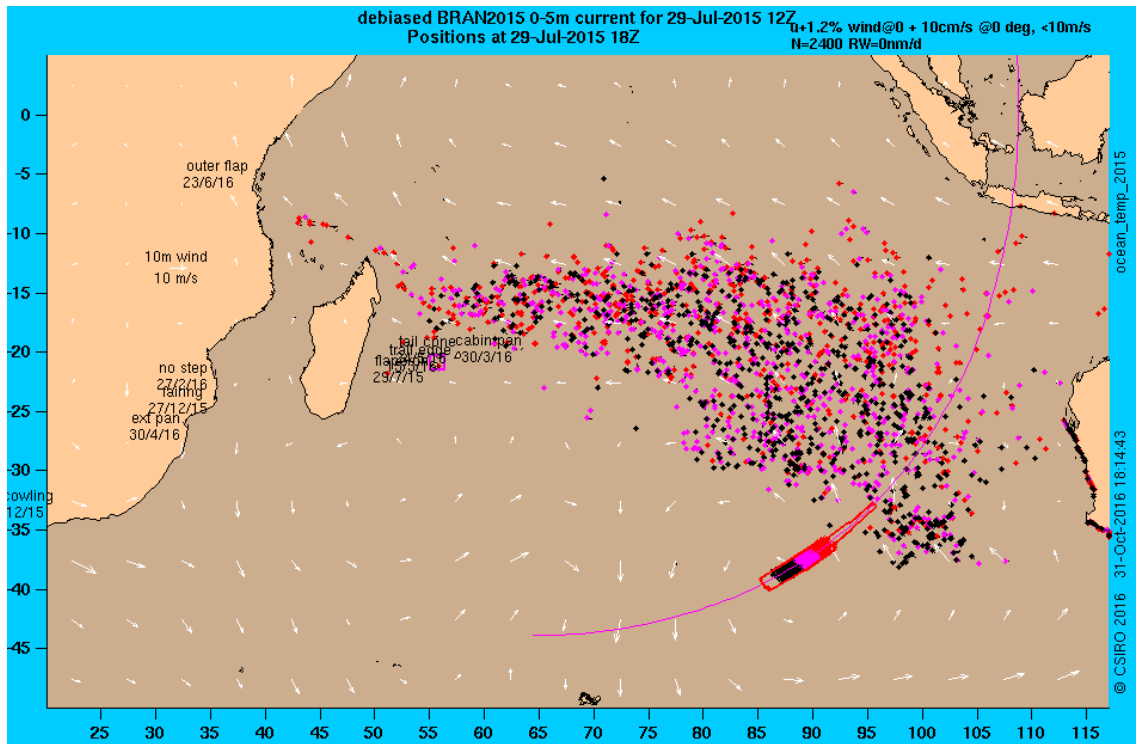
Source: CSIRO

Figure 9: Simulated location of undrogued drifters after 500 days
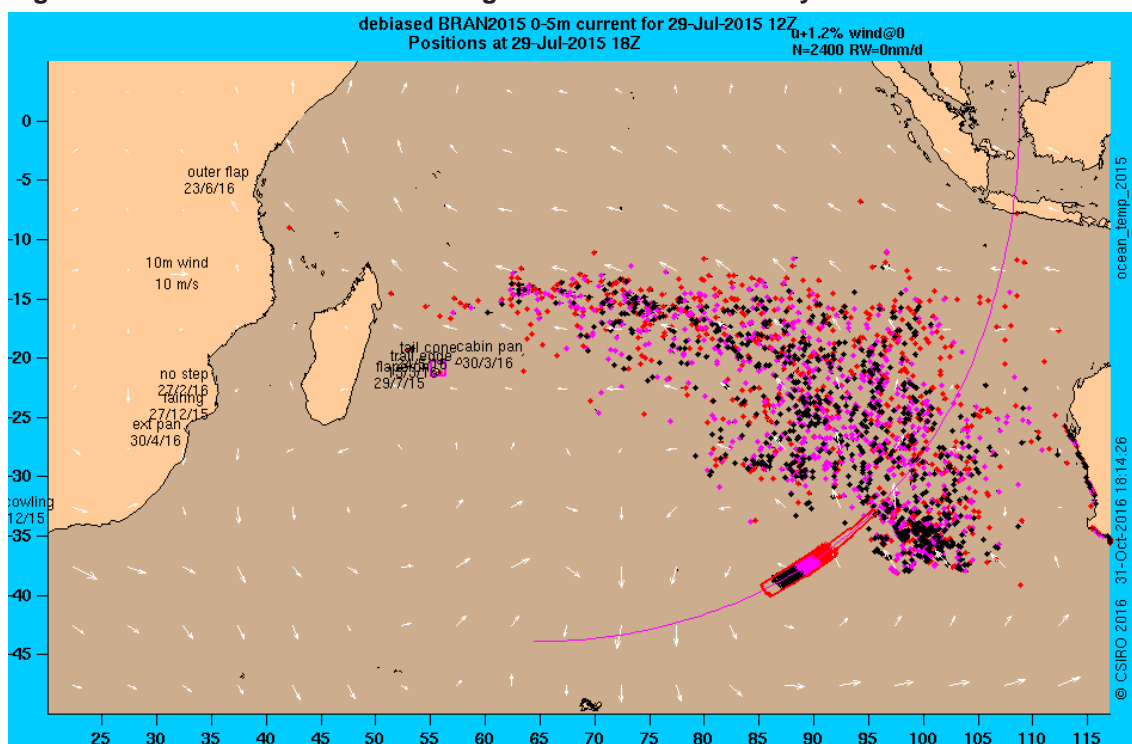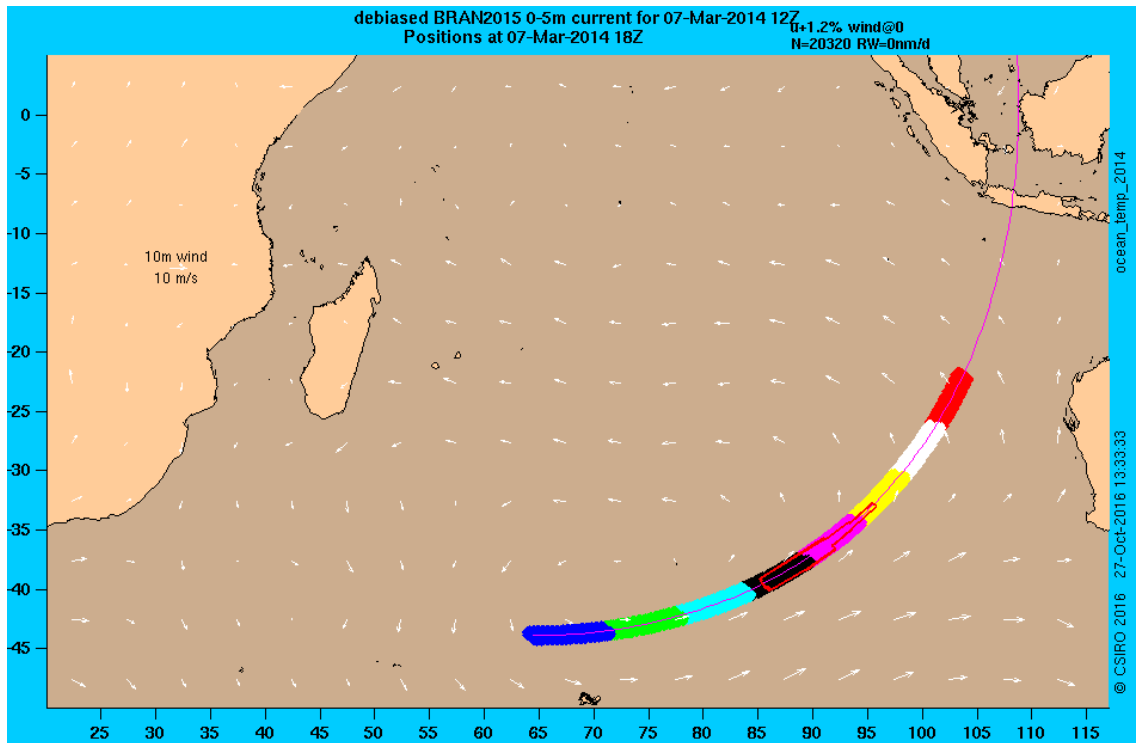

Source: CSIRO

Small errors in the simulation can result in large divergences over time. As such, an examination of the debris behaviour in the first months after the accident was conducted.

Figure 10 illustrates the starting location of the simulated drifters along the 7th arc. After eight months of simulated drift (Figure 11), some initial conclusions can be drawn about the drifter's path with respect to debris discovered to date. A significant number of drifters arrived on the coast of Western Australia. Similarly, a number of drifters had arrived on the coast of Africa. The colour of each drifter identifies its starting location as marked along the arc.

- Drifters starting in the southern half of the current search area or below (dark blue, green, light blue) can be observed on and around the coast of Western Australia, with many drifting towards Tasmania. No debris has been discovered on the Australian coast. This indicates that a starting location within the current search area, or further north, is more likely.
- A significant number of red drifters have already reached the coast of Madagascar and mainland Africa. This is not consistent with the time at which debris was discovered. The first item of debris was not discovered on Reunion Island until 16 months after the accident. This suggests a reduced likelihood of debris originating from the northernmost areas shown in Figure 10 (red and white coloured regions).

Refinement of the drift analysis is continuing. Flaperon replicas are currently deployed in the open ocean along with drogued and undrogued drifters, and replicas of smaller debris. This is to study the longer-term drift behaviour of the parts in conditions similar to those expected in the Indian Ocean. The long-term tests may provide additional improvement to the simulations and confidence in the backtracking results.

Figure 10: Simulated starting location of undrogued drifters

Source: CSIRO

Figure 11: Simulated location of undrogued drifters after 8 months
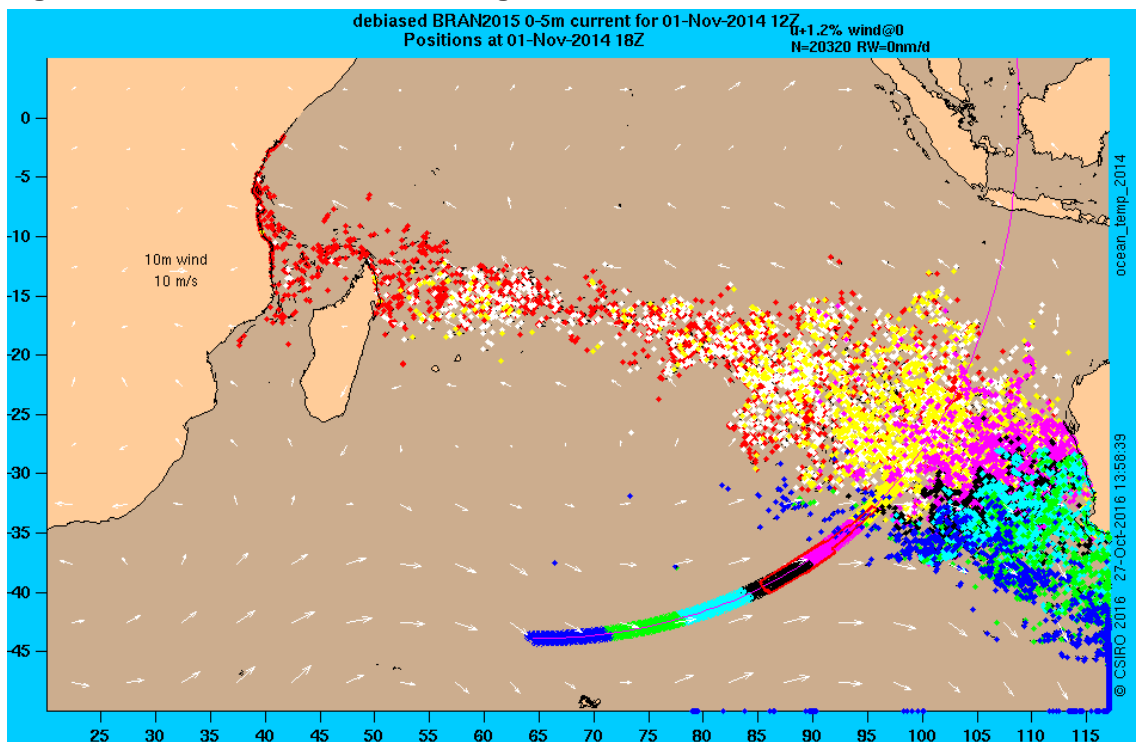
Source: CSIRO

A significant number of drifters from the light blue and green areas have made landfall on the West Australian coast. Similarly, drifters from the red and white areas have begun to make landfall on the African coastline. Neither are consistent with times and/or locations at which MH370 debris was discovered, therefore reducing the likelihood of debris originating from these locations.

Debris summary and analysis

Currently, more than 20 items of debris have been brought to the attention of and are of interest to the investigation team. The items have been located along the east and south coast of Africa, the east coast of Madagascar and the Islands of Mauritius, Reunion and Rodrigues in the Indian Ocean. A list of items recovered was published by the Malaysian investigation team and can be found at www.mh370.gov.my/index.php/en/.

The right flaperon has been examined by the French Judiciary and confirmed to have originated from 9M-MRO. Six further items of debris have previously been examined by the ATSB, comprising a:

- section of the right outboard flap fairing
- panel section from the right horizontal stabiliser
- piece of engine cowling
- closet panel section from the closet adjacent to door R1
- inboard section of the right outboard flap
- trailing edge section of the left outboard flap.

Both flap sections had unique identification numbers that were able to be linked, through manufacturing records, to 9M-MRO. The remaining examined items were confirmed as Boeing 777 parts and had identifying features linking them to a Malaysian Airlines origin, however there were no unique identifiers to link the parts directly to 9M-MRO. The parts were therefore determined to have *almost certainly* originated from 9M-MRO, given that the likelihood of originating from another source is very remote. The ATSB debris examination reports are available at www.atsb.gov.au/mh370-pages/updates/reports/.

Outboard flap failure analysis

The recovered right, outboard wing flap section (Figures 12, 13 and 14) was examined for any evidence of interaction with mechanisms, supports and surrounding components that may indicate the state of flap operation at the time of fracture and separation from the wing. The purpose of the examination was to inform the end-of-flight scenarios being considered by the search team. The most significant items of evidence in relation to this are documented below.

Figure 12: Location of recovered outboard flap section
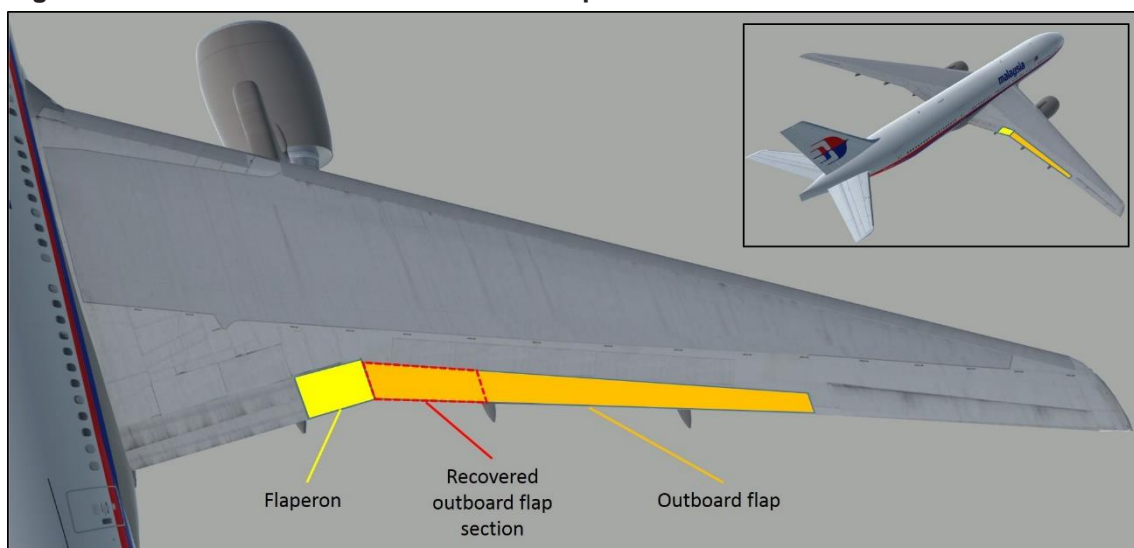
Source: DST Group (Modified by ATSB)

Figure 13: Inboard section of outboard flap

**Figure 14: Inboard section of outboard flap (inverted)**

Flap position

The trailing edge outboard wing flaps form part of the aircraft's high-lift control system and are deployed to alter the shape of the aircraft wing, improving lift at lower aircraft speeds during takeoff, approach and landing. The outboard wing flaps have defined stages of flap deployment between 'up' (retracted / cruise position) and 30-units of extension (landing position).

A fibreglass and aluminium seal pan is located at the inboard end of the outboard flap. It houses the inboard auxiliary support, comprising a deflection control track (support track) and carriage assembly. The support track is affixed to the rear of the wing. Using rollers in the carriage assembly, the inboard end of the flap is guided along the support track as the flap moves through its deflection range. The track is fully inserted into the flap in the 'up' position and progressively withdrawn from the flap as the flaps are deployed (Figure 15). The inboard auxiliary support track and carriage assembly were not present with the recovered debris.

Two adjacent aluminium stiffeners within the inboard seal pan area exhibited impact damage. The damage was significant because it was indicative of impact damage and the only component in the vicinity of the stiffeners, capable of independent movement within the seal pan, was the support track. Measurements of the support track position at the various stages of flap deployment, indicated that the track would have to be fully inserted into the flap in the retracted position to be adjacent to the damaged stiffeners (Figures 16, 17 and 18).

An outwards-fracture of the fibreglass seal pan initiated at a location adjacent to the damaged aluminium stiffeners (Figure 19). The damage was most likely also caused by impact from the support track. That damage provided further evidence of the support track position within the flap seal pan cavity, indicating that the flaps were retracted at the point of fracture and separation from the wing.

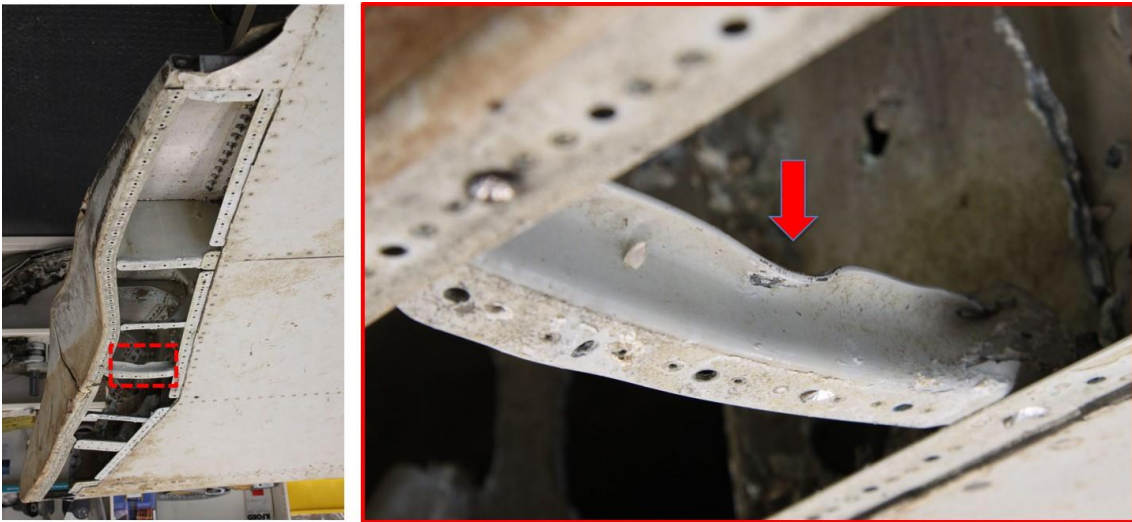**Figure 15: Outboard flap, inboard auxiliary support**
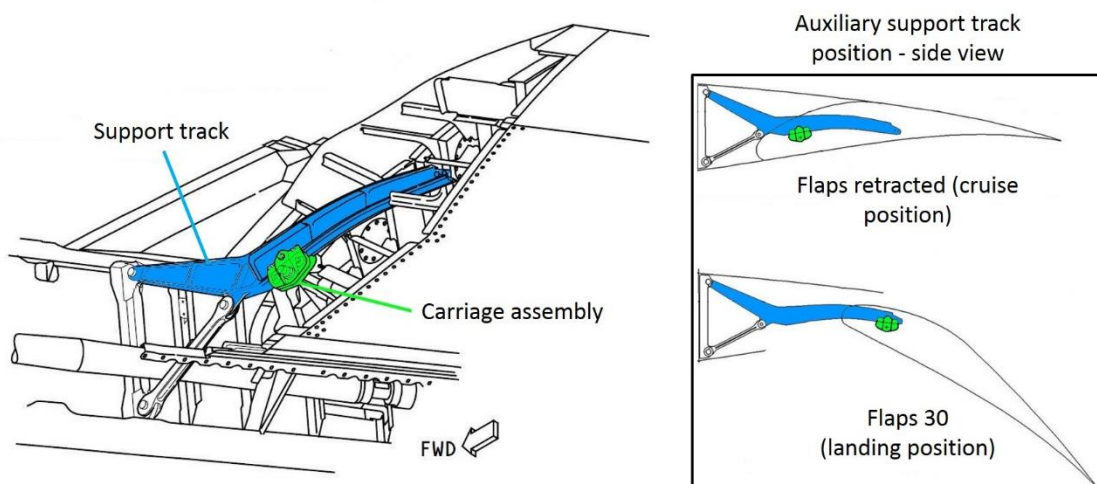
Source: Boeing (modified by ATSB)

Figure 16: Outboard flap location of damaged stiffeners within the seal pan cavity
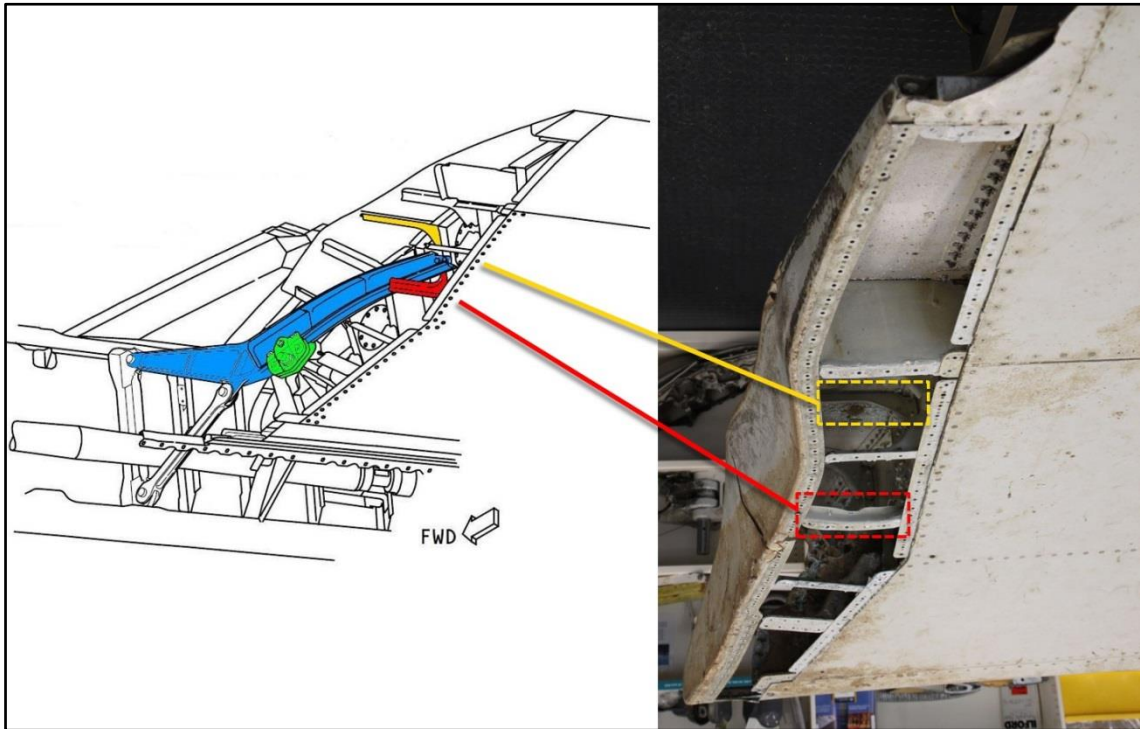
Source: Boeing (modified by ATSB) / ATSB

Figure 17: Outboard flap, damaged stiffeners within the seal pan cavity

Source: ATSB

Figure 18: Outboard flap, damaged stiffeners within the seal pan cavity

Source: ATSB

Figure 19: Outboard flap, fractured seal pan (forward)

Source: ATSB

Contact damage between the flaperon and outboard flap

The flap seal pan was also fractured adjacent to the rear spar. The fracture resulted from external impact, puncturing the fibreglass and plastically deforming the supporting aluminium structure within the seal pan cavity (Figure 20). Comparable damage was noted at the outboard, rear spar and surrounding structure of the adjacent flaperon (Figure 21). It was noted that the two areas in question are aligned when the flaps are in the retracted position, with a significant offset existing at other stages of flap extension (Figure 22).

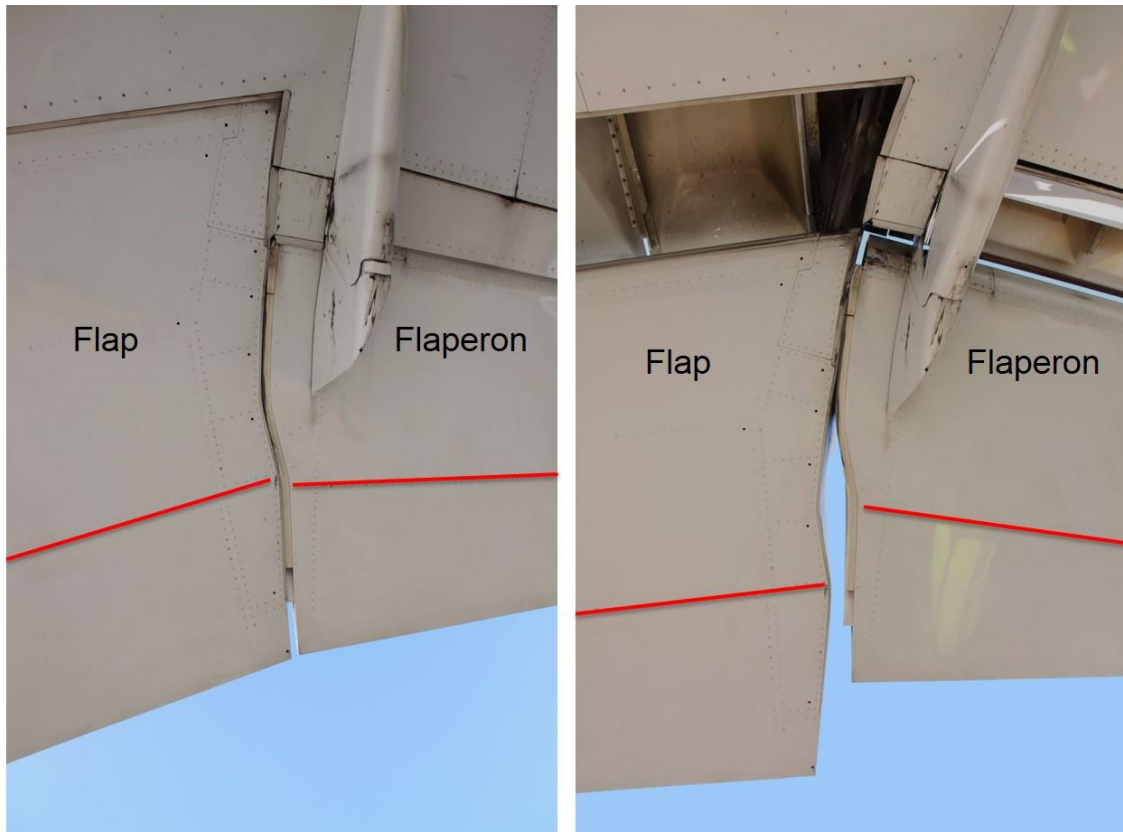**Figure 20: Outboard flap, fractured seal pan (aft)**

Source: ATSB

Figure 21: Flaperon, outboard side damage

Source: Direction générale de l'armement / Techniques aéronautiques (modified by ATSB)

Figure 22: Flaperon and outboard flap from below, showing relative alignment of rear spar rivet line (highlighted) in the flaps retracted (left) and extended position (right)

Source: ATSB

Analysis

Damage to the internal seal pan components at the inboard end of the outboard flap was possible with the auxiliary support track fully inserted into the flap. That damage was consistent with contact between the support track and flap, with the flap in the retracted position. The possibility of the damage originating from a more complex failure sequence, commencing with the flaps extended, was considered much less likely.

With the flap in the retracted position, alignment of the flap and flaperon rear spar lines, along with the close proximity of the two parts, indicated a probable relationship between two areas of damage around the rear spars of the parts. This was consistent with contact between the two parts during the aircraft breakup sequence, indicating that the flaperon was probably aligned with the flap, at or close to the neutral (faired) position.

Numerous other discrete areas of flap damage were analysed. Some of the damage was consistent with the flaps in the retracted position, while other areas did not provide any useful indication of the likely flap position. It was therefore concluded that:

- The right outboard flap was most likely in the retracted position at the time it separated from the wing.
- The right flaperon was probably at, or close to, the neutral position at the time it separated from the wing.

Acknowledgements

The ATSB would like to acknowledge the following organisations for their input and continued assistance with the analysis:

- Air Accidents Investigation Branch (UK)
- Australian Bureau of Meteorology
- Australian Defence Science and Technology Group
- Boeing
- Commonwealth Scientific and Industrial Research Organisation
- Department of Civil Aviation, Malaysia
- Inmarsat
- Malaysian Airlines Berhad
- Malaysian Ministry of Transport
- National Transportation Safety Board (US)
- Thales.

Those involved have dedicated many hours outside of normal duties to advance the collective understanding of the event. The main focus has always been in finding the aircraft to assist the Malaysian investigation team and to bring closure to the families of the passengers and crew of MH370.